*Electroencephalography and clinical Neurophysiology*, 1991, 78: 389–401
© 1991 Elsevier Scientific Publishers Ireland, Ltd. 0013-4649/91/$03.50
*ADONIS* 0013464991000956

1991

EEG 89260

# Fluctuations of steady-state VEPs: interaction of driven evoked potentials and the EEG

Joelle Mast [a] and Jonathan D. Victor [a,b]

[a] *Department of Neurology and Neuroscience, Cornell University Medical College, New York, NY 10021 (U.S.A.), and* [b] *Laboratory of Biophysics, The Rockefeller University, New York, NY 10021 (U.S.A.)*

(Accepted for publication: 6 July 1990)

Summary

We performed a detailed analysis of the variability of a steady-state human evoked potential (EP) and the spectral properties of the simultaneously recorded electroencephalogram (EEG). This allowed us to determine whether the background EEG was influenced by the evoked potential stimulus, and to what extent variability of evoked potential estimates is simply due to the addition of the background EEG.

Steady-state visual evoked potentials (VEPs) were elicited by a checkerboard undergoing contrast-reversal modulation at 1 of 3 fundamental frequencies f: 5.0 Hz, 7.5 Hz, and 10.0 Hz. To a first approximation, the evoked potential (at frequency 2 f) and the undriven components of the EEG combined linearly. However, two kinds of interactions were present: (i) patterned visual stimulation decreased the power in the undriven EEG in the 5–17 Hz range by as much as a factor of 2; (ii) superimposed on this overall effect of pattern stimulation, there were changes in the EEG power at specific harmonics of the input frequency. Power increased by as much as 6-fold at the stimulus reversal rate (2 f) and its second harmonic (4 f). These findings imply a complex non-linear interaction between the visual input and the EEG.

Key words: Fourier analysis; Power spectrum; Visual evoked potentials

An evoked potential (EP) is the summation of individual cellular events synchronized to an external stimulus. EPs are typically measured either by averaging the surface potential recorded during many repetitions of a stimulus or by Fourier analysis. Potentials due to cellular events locked to the stimulus are reinforced by the averaging process. Potentials due to cellular events uncorrelated with the stimulus are not reinforced by the averaging process, and are attenuated (under ideal circumstances) in proportion to the square root of the number of averages.

Signals uncorrelated with the stimulus are 'noise' in the sense that they contribute to variability of the estimated averaged EP. Typical procedures for extracting EPs seek to minimize the contribution of these signals. However, as has been recognized since the early days of EP recordings (see Regan 1989 for a review), these signals may be in part dependent on the stimulus, and may provide additional information concerning brain processes. We will call alterations of brain activity which are due to the stimulus but not extracted by averaging techniques the 'undriven' components of the EP. Signals that are extracted by averaging techniques, i.e., the traditional EP, will be called the 'driven' components of the EP.

On a practical level, the undriven components of the EP, if present, would be manifest as a source of variability in studies designed to extract the driven EP. Thus, a better understanding of undriven EP components may lead to improved methods of signal processing analysis for extraction of the driven EP components, and more rigorous statistical techniques for quantifying their size (Victor and Mast 1991).

The null hypothesis for our analysis is that the variability in estimates of the visual EP (VEP) is due to incomplete suppression of the electroencephalogram (EEG) in the averaged record. That is, we postulate that there are no undriven VEP components, and that all of the variability of the VEP is accounted for by the statistics of the EEG that would be recorded during fixation of an unmodulated display. This hypothesis merely formalizes the idea that the visual stimulus affects only a small number of neurons, and does not influence bulk brain activity. As shown in the theoretical section of Methods, this hypothesis predicts that the power spectrum measured in the presence of periodic visual stimulation is identical to the power spectrum of the EEG measured during fixation of an unmodulated display.

*Correspondence to:* Jonathan D. Victor, Cornell University Medical College, 1300 York Avenue, New York, NY 10021 (U.S.A.).

We will find that this prediction of the null hypothesis is false. Rather, a periodic visual stimulus influences bulk brain activity not only by producing an averaged VEP, but also by alterations of the background EEG. Some, but not all, of these changes may be related to non-specific effects of attention and arousal. The nature of these alterations allows us to draw some qualitative inferences concerning the dynamics of VEP generation.

## Methods

*Physiological methods*

Eight adult subjects aged 25–35 (the authors and 6 healthy volunteers) with normal or corrected-to-normal vision participated in this study. The visual stimulus was a checkerboard whose checks subtended 16 min at a contrast $[(I_{max} - I_{min})/(I_{max} + I_{min})]$ of 0.4. Episodes consisted of sinusoidal counterphase modulation of the contrast of the checkerboard stimulus at fundamental frequencies (f) of 5.0 Hz, 7.5 Hz, and 10.0 Hz. (Reversal frequencies, at which pattern-reversal EP components were expected, corresponded to 2 f: 10.0 Hz, 15.0 Hz, and 20.0 Hz.) A fourth kind of episode consisted of presentation of a static checkerboard at the contrast of 0.4; the subject was instructed to maintain fixation of the center of the unmodulated display during the course of this episode. The checkerboard had a mean luminance of 128 cd/m$^2$ and subtended an 8.8° visual angle at the viewing distance of 57 cm. All stimuli were produced on a Tektronix 608 CRT (P31 phosphor) whose control signals (X-deflection, Y-deflection, and Z (intensity)) where generated by specialized electronics (Milkman et al. 1980) interfaced to a DEC 11/73 computer. The electronics of the display controller provided for linearization of the intensity/voltage characteristic of the CRT.

Scalp signals were recorded at $O_z$-$C_z$ via gold cup electrodes applied to the scalp with Nihon-Kohden electrolyte paste, amplified 10,000-fold, bandpass-filtered (1–100 Hz) by a high-impedance isolation amplifier, and digitized at the stimulus frame rate of 270 Hz by the 11/73 computer. One episode of data collection consisted of 30 sec. Each subject sat for a total of 32 trials (8 at each of the 3 temporal frequencies and 8 trials of a static checkerboard). Trials were presented in a randomly interleaved fashion. Breaks were provided as needed by the subjects to maintain concentration.

Digitized data were saved for later analysis *without* averaging. Thus, in the off-line analysis, we were able to calculate Fourier components at the frequencies of interest (the reversal frequency, its harmonics, and its subharmonics) for arbitrary subsegments of each episode. As seen below, this allowed us to investigate the statistics of the steady-state VEP estimates.

*Analytical methods*

Our method for spectral estimation, described here, allowed estimation of spectral components even at the stimulation frequency itself. Comparisons of power spectra obtained with and without periodic visual stimulation allow us to test whether the variability in the measured VEP is simply the result of the addition of a fixed background 'noise' to the VEP signal. Spectral estimates are obtained by (i) segmentation of the data, (ii) calculation of Fourier components from each segment, and (iii) estimation of the scatter of each Fourier component about its mean, *without* assuming that the mean is zero. Here we briefly formalize this method for spectral estimation and demonstrate that it provides proper estimates of the spectrum of an additive noise, even in the presence of a periodic signal. More details concerning this algorithm are considered in the Appendix.

Let us represent the recorded scalp signal by S(t). We will form an estimate of its power spectrum $\hat{S}(\omega)$ from Fourier transforms of S(t) over finite samples of data. For a sample of data of length L centered at a time T, we denote the cosine and sine components of the Fourier transform of S(t) at the frequence $\omega$ by $x_S(\omega,L,T)$ and $y_S(\omega,L,T)$:

$$\left.\begin{aligned} x_S(\omega,L,T) &= \int_{-\infty}^{\infty} S(t)\, W(t-T)\cos(\omega t)\, dt \\ y_S(\omega,L,T) &= -\int_{-\infty}^{\infty} S(t)\, W(t-T)\sin(\omega t)\, dt \end{aligned}\right\} \quad (1)$$

where W(t) is a normalized window function

$$W(t) = 1/L \text{ if } |t| \leq L/2;\ W(t) = 0, \text{ otherwise.} \quad (2)$$

We restrict attention to frequencies $\omega$ which repeat an integral number of times in the analysis period L. We further assume that the analysis period L is an integer multiple of the stimulus period P.

It is convenient to consider the two real Fourier estimates $x_S(\omega,L,T)$ and $y_S(\omega,L,T)$ together, as an estimate of a single complex Fourier component:

$$z_S(\omega,L,T) = x_S(\omega,L,T) + \imath y_S(\omega,L,T)\rangle. \quad (3)$$

The deviation of an individual estimate of $z_S(\omega,L,T)$ from its expected value $\langle z_S(\omega,L,T)\rangle$ will be denoted by

$$\delta z_S(\omega,L,T) = z_S(\omega,L,T) - \langle z_S(\omega,L,T)\rangle. \quad (4)$$

The power spectrum $\hat{S}(\omega)$ is related to the variance of $\delta z_S(\omega,L,T)$ by

$$\hat{S}(\omega) = \lim_{L\to\infty} \frac{L}{2\pi} \langle |\delta z_S(\omega,L,T)|^2 \rangle. \quad (5)$$

In the above equations (4) and (5), the brackets $\langle\ \rangle$ indicate the expected value of the quantity they enclose. Strictly speaking, this expected value is an average to be calculated over a statistical ensemble of instances of the

experiment. In practice, this ensemble average is replaced by an average over multiple data segments, each centered at time $T_j$. The times $T_j$ must all be at the same phase of the external stimulus. That is, we calculate

$$\langle z_S(\omega,L,T)\rangle_{est} = \frac{1}{J}\sum_{j=1}^{J} z_S(\omega,L,T_j) \qquad (6)$$

and

$$\langle |\delta z_S(\omega,L,T)|^2\rangle_{est} = \frac{1}{J-1}\sum_{j=1}^{J} |z_S(\omega,L,T_j) - \langle z_S(\omega,L,T)\rangle_{est}|^2. \qquad (7)$$

In the limit that the number of estimates J is large, the estimated quantities in equations (6) and (7) become equal to their exact values, which appear in equations (4) and (5). The quantity $J-1$ appears in the denominator of (7) rather than the quantity J, because the average value of $\langle z_S(\omega,L,T)\rangle$ is estimated from the data, rather than assumed to be zero. If the quantities $z_S(\omega,L,T_j)$ are independent (see Appendix), then there are $2(J-1)$ degrees of freedom associated with the estimate (7): $J-1$ degrees of freedom for the contributions of the real parts, and $J-1$ degrees of freedom for the contribution of the imaginary parts. Note that for contiguous data which have been segmented into segments of length L, $\langle z_S(\omega,L,T)\rangle_{est}$ can be calculated either as an average of individual Fourier estimates (as indicated by eqn. 6), or as a single Fourier estimate obtained from the unsegmented record.

Now let us assume that the signal S(t) is a sum of two components: an evoked response, R(t), and ongoing 'noise' unrelated to the stimulus, E(t):

$$S(t) = R(t) + E(t) \qquad (8)$$

E(t) represents not only endogenous EEG, but also exogenous sources of variability, such as signals generated by head movement. The expected value of the 'noise' E(t) is assumed to be equal to zero. The 'true' evoked response R(t) is assumed to be a periodic function with period P (the stimulus period), and to have no intrinsic variability. We will show that application of the algorithm (7) to S(t) yields a power spectrum $\hat{S}(\omega)$ which is equal to the power spectrum of the 'noise,' $\hat{E}(\omega)$.

Since the VEP signal R(t) and the EEG 'noise' R(t) combine additively, so do their Fourier components (1):

$$z_S(\omega,L,T) = z_R(\omega,L,T) + z_E(\omega,L,T). \qquad (9)$$

It follows that fluctuations of these Fourier components about their mean values are also additively related:

$$\begin{aligned} z_S(\omega,L,T) &- \langle z_S(\omega,L,T)\rangle_{est} \\ &= [z_R(\omega,L,T) - \langle z_R(\omega,L,T)\rangle_{est}] \\ &\quad + [z_E(\omega,L,T) - \langle z_E(\omega,L,T)\rangle_{est}] \\ &= [z_E(\omega,L,T) - \langle z_E(\omega,L,T)\rangle_{est}]. \end{aligned} \qquad (10)$$

The second equality follows from the fact that the response R(t) is assumed to be deterministic, and thus its Fourier components $z_R(\omega,L,T)$ are equal to their mean values $\langle z_R(\omega,L,T)\rangle_{est}$.

It follows from (10) that estimates of the variance of the combined VEP and EEG signal $\langle |\delta z_S(\omega,L,T)|^2\rangle_{est}$ as derived from (7) are equal to the estimates of the variance of the EEG signal alone $\langle |\delta z_E(\omega,L,T)|^2\rangle_{est}$ derived by the same procedure. Since the power spectrum is related to these variance estimates through equation (5), the power spectrum $\hat{S}(\omega)$ as estimated by this method is equal to $\hat{E}(\omega)$, the power spectrum of the 'noise' E(t) in isolation.

We contrast the algorithm summarized by equations (5), (6) and (7) with the more traditional approach (Kay 1988) to spectral estimation, which is applicable when the signal S(t) does not contain periodic components. In this case, $\langle z_S(\omega,L,T)\rangle$ is *assumed* to be zero, rather than estimated from the data by equation (6). In this case, (7) is replaced by

$$\langle |\delta z_S(\omega,L,T)|^2\rangle_{est} = \frac{1}{J}\sum_{j=1}^{J} |z_S(\omega,L,T_j)|^2. \qquad (11)$$

This estimate of $\langle |\delta z_S(\omega,L,T)|^2\rangle$ does *not* yield a convergent estimate of the power spectrum (5), if there are periodic components in S(t). Rather, as the analysis period L increases, spectral estimates obtained from (11) have progressively higher and narrower peaks at the frequency of any periodic input.

## Results

The simplest hypothesis concerning fluctuations of the steady-state VEP is that fluctuations are solely due to superimposed background EEG, incompletely suppressed by the averaging process. Implicit in this view is the hypothesis that the background EEG is independent of whether or not periodic visual stimulation is present: the basic notion is that the VEP simply adds to an ongoing process. As seen above, this implies that spectral estimates should be independent of whether visual stimulation is present. We now test this prediction.

Since we do not explicitly consider the limiting process $L \to \infty$ of equation (5), we are (strictly speaking) examining variances of estimates of Fourier components, rather than power. Power spectral estimates are readily obtained from variances of Fourier components, through a normalization for epoch duration (5). Because of this relationship, variance ratios are identical to ratios of spectral estimates.

### *Relation of the spectrum of the background EEG to visual stimulation*

Estimated values of the variance

$(V(f) = \langle |\delta z_S(2\pi f, L,T)|^2\rangle_{est}$ (equation (7))

were calculated as a function of temporal frequency f for the 4 experimental conditions: 5 Hz stimulation, 7.5 Hz stimulation, 10 Hz stimulation, and static stimulation. The interval length L used for analysis was the entire episode length (29.96 sec), so that the resolution of each frequency bin was 0.03 Hz. At each frequency, a geometric mean across subjects was calculated. (Geometric, rather than arithmetic, means are used to avoid bias towards the behavior of subjects who happened to have a large EEG amplitude, and also because the ultimate quantities of interest are variance *ratios*.) The resulting variance estimates, smoothed by averaging (arithmetically) across frequency windows of 1.0 Hz (30 frequency bins) are shown in Fig. 1.

Though the variances in the static condition (solid circles) are similar to those in the 3 conditions of periodic stimulation, several differences are apparent. For analysis frequencies f in the range 5–17 Hz, stimulation systematically reduced the variance. The 10 Hz stimulation frequency (inverted triangles) had the largest effect, followed by the 7.5 Hz stimulation frequency, followed by the 5 Hz stimulation frequency. The peak effect occurred at analysis frequencies in the alpha range and amounted to a power attenuation by a factor

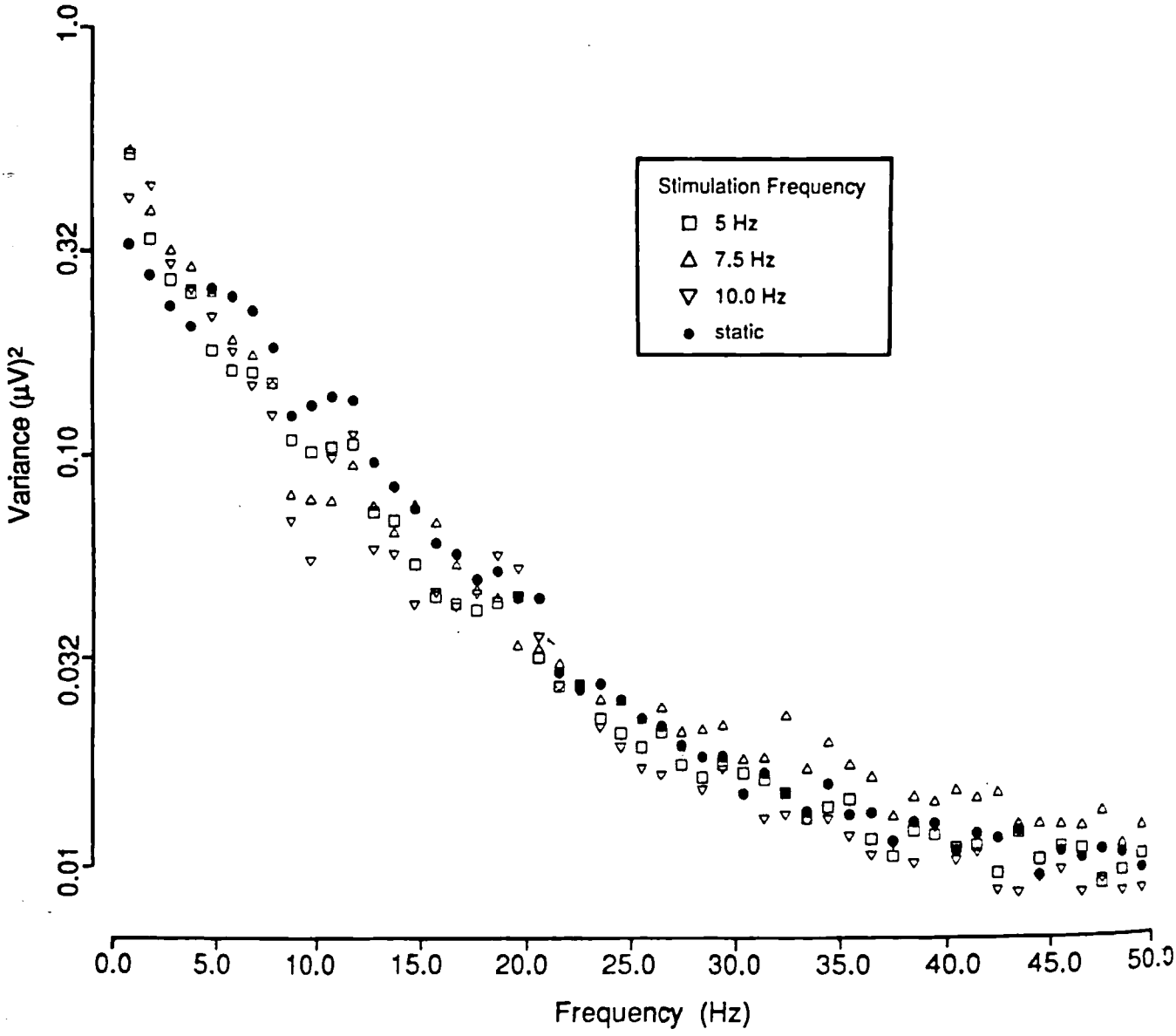


Fig. 1. Smoothed variances of EEG Fourier components with and without periodic visual stimulation. The Fourier components are calculated over a 29.96 sec episode, and variances are estimated within each of the 8 subjects. The geometric means across subjects are plotted for stimulation at 5.006 Hz (open squares), 7.509 Hz (open triangles), and 10.012 Hz (open inverted triangles), and for static stimulation (filled circles). Each data point represents the arithmetic mean of 30 adjacent frequency bins. Variances are in $\mu V^2$.

of 2.4 at 9 Hz. That these findings are not likely to be due to chance is readily seen from their consistency across analysis frequencies.

Below 5 Hz, there was an increase in variance with contrast-reversal stimulation, without clear dependence on the stimulation frequency. The maximum size of the effect was an increase in power by a factor of 1.6. Above 20 Hz, variance in the static condition and the 5 Hz stimulation conditions were similar. There was a slight tendency for increased variance with 7.5 Hz stimulation, and decreased variance with 10 Hz stimulation. The effects of periodic stimulation on variances above 20 Hz were very small, typically 15% or less.

At the frequency resolution in Fig. 1, the major effect of stimulation was to depress variance in the 5–17 Hz range; the amount of depression depended on the input frequency. At a higher frequency resolution of 0.03 Hz (Fig. 2), other phenomena appeared. For all 3 modulated stimuli (Fig. 2A, B, C), a peak of width approximately 0.5 Hz centered at approximately 11 Hz was present. There was little evidence of this peak in the unstimulated condition (Fig. 2D). Detailed comparison of stimulated and unstimulated spectra reveal that this peak does not represent an increase in variance with stimulation, but rather, less stimulus-dependent variance loss at 11 Hz than at neighboring frequencies. Whether this phenomenon reflects a special interaction with the alpha rhythm per se cannot be determined from our data.

The major finding seen in the high-resolution spectra is that there are increases in the variance at frequencies harmonically related to the stimulus frequency. With $f = 5.006$ Hz stimulation, there are one-bin peaks at exactly $2f = 10.012$ Hz and $4f = 20.024$ Hz. With $f = 7.509$ Hz stimulation, there is a one-bin peak at exactly $2f = 15.018$ Hz and a less-prominent peak at $4f = 30.036$ Hz. Similar peaks at 2f and 4f appear with stimulation at $f = 10.012$ Hz. It can be seen that all of these peaks are highly unlikely to be due to chance alone, in that they are larger in amplitude than their hundred or so neighbors. There was no increase in variance at frequencies removed from 2f or 4f by as little as 0.03 Hz.

To assess the statistical significance of these data, we cannot simply use the $F$ distribution for individual variance ratios, since the quantities we have plotted are geometric means of variance ratios from several ($N = 8$) subjects. However, we may proceed as follows: for gaussian-distributed quantities, variance estimates with

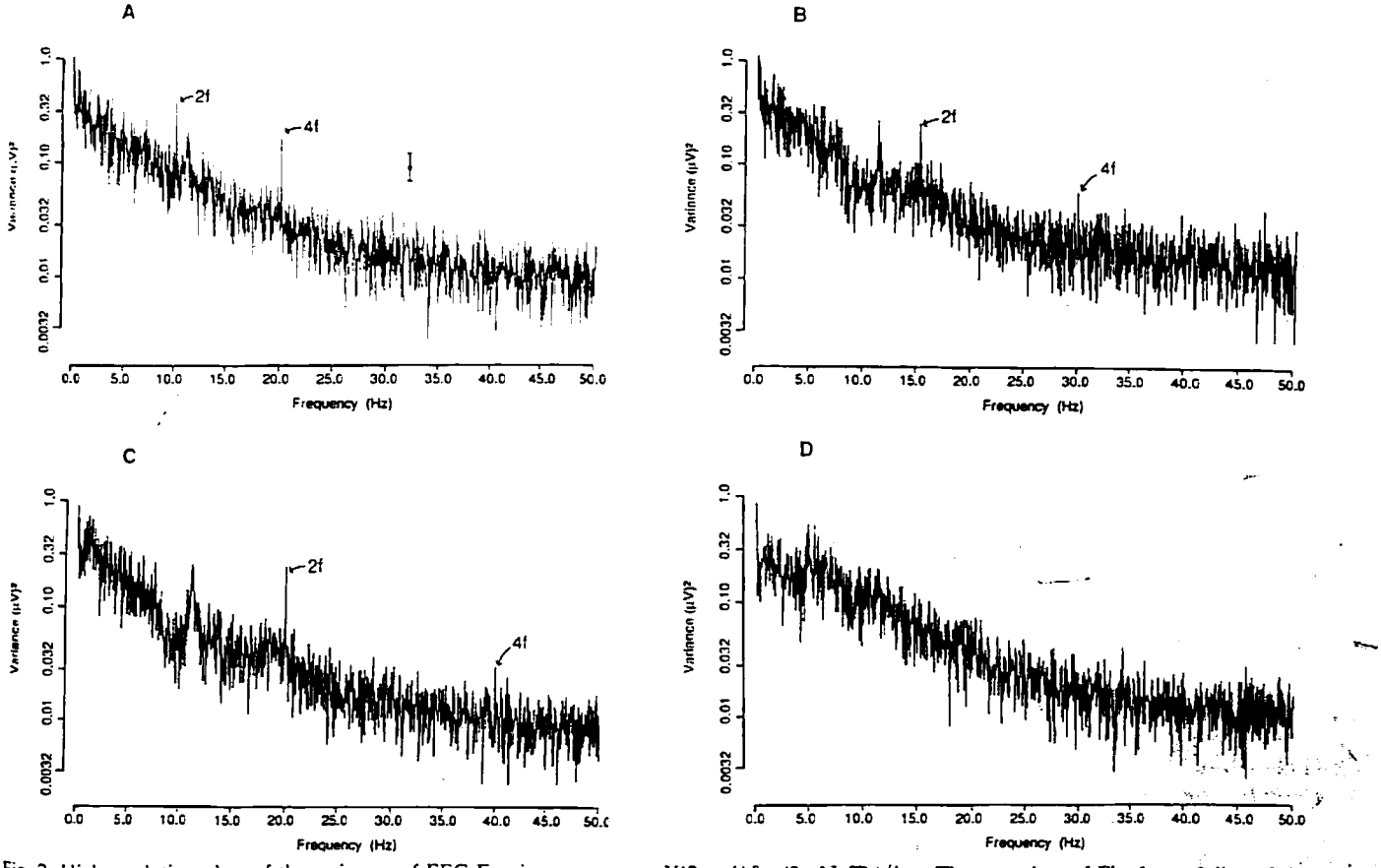


Fig. 2. High-resolution plots of the variances of EEG Fourier components $V(f) = \langle |\delta z_S(2\pi f, L, T)|^4 \rangle_{est}$. The procedure of Fig. 1 was followed, but variance estimates within individual 0.03 Hz bins are retained. A: stimulation at 5.006 Hz. B: stimulation at 7.509 Hz. C: stimulation at 10.012 Hz. D: static stimulation. Variances are in $\mu V^2$. The calibration bar indicates a 95% confidence interval, calculated as described in the text.

n degrees of freedom have a variance equal to 2/n times the sample variance (asymptotically for large n). It follows that the logarithm of a variance estimate has a variance of 2/n (asymptotically for large n). For a logarithm of a ratio of independent variance estimates, the variances add. Thus, if numerator and denominator have $n_1$ and $n_2$ degrees of freedom respectively, their ratio has variance $2/n_1 + 2/n_2$. The mean of N such log-ratios has variance $[2/n_1 + 2/n_2]/N$. For large $n_1$, $n_2$, and N, this quantity (the mean log-ratio) is gaussian-distributed, according to the central limit theorem. In our application, $n_1 = n_2 = 14$, the number of degrees of freedom in a variance estimate in one subject, N = 8, the number of subjects. Thus, the logarithm of the quantity plotted in Fig. 2 is approximately gaussian-distributed with variance 1/28. 95% confidence limits are then obtained from standard tables of the normal distribution.

*Nature of the stimulus frequency-specific increase in variance*

We now turn to an analysis of the increase in variance at harmonics of the input frequency. In order to remove the overall effect of periodic stimulation on the variance (Fig. 1), we compare variance estimates at harmonics kf of the input frequency f to variance estimates at nearby frequencies $kf + \delta$ and $kf - \delta$, with $\delta = 0.03$ Hz. For each subject, we calculated G(k,f), where

$$G(k,f) = V(kf)/[V(kf - \delta)V(kf + \delta)]^{1/2}. \qquad (12)$$

G(k,f) thus represents the proportional height of the variance peak at kf, referred to its local baseline.

Geometric means of G(k,f) across the 8 subjects are shown in Table I. The 95% confidence limits of this quantity are 0.725–1.378, calculated as described above. All even harmonics up to 30 Hz show an enhancement of variance. This enhancement is most prominent for frequencies kf in the neighborhood of 20 Hz: the largest effect for the input frequency f = 5 Hz is seen at its fourth harmonic (k = 4), while the largest effect for the input frequency f = 10 Hz is seen at its second harmonic (k = 2). No clear evidence of a change in response variance is seen at the input frequency itself (k = 1). However, there is a statistically significant suppression of variance at k = 3 for two of the input frequencies and an enhancement of variance at k = 5 for all input frequencies.

Now, let us focus on the variance increase at 2f, which is clearly seen for all 3 input frequencies studied (Fig. 2A–C and Table I). The variance of a (complex) Fourier component is described by 3 quantities: the variance of the real part, denoted $V_{xx}$, the variance of the imaginary part, denoted $V_{yy}$, and the covariance of the real and imaginary parts, denoted $V_{xy}$. These quantities are not the most useful ones for some analytical purposes, however. We therefore consider two derived quantities. One is the ratio of the variance of the real part to the variance of the imaginary part, denoted $F = V_{xx}/V_{yy}$. For gaussian noise, it is distributed like an $F$ statistic with n − 1 degrees of freedom in numerator and denominator. The second is the correlation coefficient of the real and imaginary parts, denoted $r = V_{xy}/(V_{xx}V_{yy})^{1/2}$. For gaussian noise, it is distributed like a standard product-moment correlation coefficient, with n − 2 degrees of freedom. Together with the overall variance $V = V_{xx} + V_{yy}$, the quantities $F$ and $r$ determine the set of partial variances and covariances $V_{xx}$, $V_{yy}$, and $V_{xy}$.

The relationship of the quantities $V_{xx}$, $V_{yy}$, and $V_{xy}$, $r$, and $F$ are illustrated in Fig. 3. The average value of a Fourier estimate $\langle z_S(\omega,L,T)\rangle$ may be regarded as a vector in the complex plane, whose length represents the magnitude of the Fourier component and whose direction represents the phase of the Fourier component. Individual estimates of this quantity will scatter in a cloud around their mean value. For any desired level of confidence, this scatter may be described by a confidence region, analogous to a confidence interval. If the variability is due to a gaussian process, the confidence region is an ellipse. In the special case (see Appendix) that the gaussian process is not synchronized to the

TABLE I

Relative variance at harmonics of the input frequency. Geometric means of the quantity G(k,f) across subjects. This quantity (equation 12) expresses the relative amount of variance at the frequency kf compared with the variance at nearby frequencies, during stimulation at the frequency f. Upward arrows denote values which lie in the upper 2.5% of their theoretical distributions, and downward arrows denote values which lie in the lower 2.5% tail of their distribution. Theoretical distributions are determined as described in the text. Columns are spaced in order to align the rows corresponding to equal output frequencies kf.

| kf | f = 5.006 Hz | f = 7.509 Hz | f = 10.012 Hz |
|---|---|---|---|
| 5.006 | k = 1: 1.276 | | |
| 7.509 | | k = 1: 1.594↑ | |
| 10.012 | k = 2: 3.792↑ | | k = 1: 0.955 |
| 12.515 | | | |
| 15.018 | k = 3: 0.864 | k = 2: 3.891↑ | |
| 17.521 | | | |
| 20.024 | k = 4: 6.562↑ | | k = 2: 4.972↑ |
| 22.527 | | k = 3: 0.375↓ | |
| 25.030 | k = 5: 1.529↑ | | |
| 27.534 | | | |
| 30.037 | k = 6: 1.864↑ | k = 4: 2.461↑ | k = 3: 0.576↓ |
| 33.540 | | | |
| 35.043 | k = 7: 0.603↓ | | |
| 37.546 | | k = 5: 1.700↑ | |
| 40.049 | k = 8: 1.163 | | k = 4: 3.183↑ |
| 42.552 | | | |
| 45.055 | k = 9: 0.308↓ | k = 6: 1.488↑ | |
| 47.558 | | | |
| 50.061 | k = 10: 1.721↑ | | k = 5: 2.261↑ |

stimulus, then the confidence region must be a circle, rather than a general ellipse. This situation is illustrated in Fig. 3A.

The quantities $r$ and $F$ describe deviations of the confidence region from a circle. $V_{xx}$ is essentially the projection of the ellipse onto the real axis, and $V_{yy}$ is essentially its projection onto the imaginary axis. Their ratio, $F$, indicates whether the confidence region is elongated horizontally ($F > 1$) or vertically ($F < 1$). Fig. 3B is an example of a confidence region with $F > 1$ and $r = 0$. The correlation coefficient $r$ indicates whether there is any interaction between real and imaginary parts of the variance. A non-zero $r$ thus means that the confidence region is elongated along a diagonal. Fig. 3C is an example of a confidence region with $F = 1$ and $r > 0$. For the typical confidence ellipse, both $F \neq 1$ and $r \neq 0$. This is shown in Fig. 3D.

Table II presents measurements of $r$ and $F$ at the second harmonic of the stimulus frequency, along with the response amplitude A(2f), the overall variance V(2f), and the ratio of the variance in the stimulated condition to the variance in the unstimulated condition, $V(2f)/V_0(2f)$.

The hypothesis of additive gaussian noise leads to simple predictions for the distribution of these derived parameters. The real and imaginary parts of the variance should be (i) equally distributed and (ii) independent (see Appendix). If equally distributed, their ratio, $F(2f)$, should be distributed according to an $F$ distribution. The number of degrees of freedom is 7, one less than the number of individual estimates in the sum (7). If independent, the correlation coefficient $r(2f)$ should be symmetrically distributed about zero according to the distribution of the product-moment correlation coefficient. The number of degrees of freedom is 6, two less than the number of individual estimates in the sum (7). These facts, along with published tables of the appropriate distributions (Sokal and Rohlf 1969), were used to determine whether the scatter of $F(2f)$ about 1, and of $r(2f)$ about 0, was anticipated from chance alone. Two of the values of $F(2f)$ lie in the lower 5% tail of the appropriate $F$ distribution, and two lie in the upper 5% tail. Out of 24 values of $F(2f)$ displayed, it would be expected that a total of 2.4 values are in these tails. Finding 4 or more values, rather than the expected 2.4, would occur at least 22% of the time, according to Poisson statistics. Similarly, out of the 24 values of $r(2f)$ displayed, one lies in the lower 2.5% tail and two lie in the upper 2.5% tail. Three or more values in the tails would occur at least 12% of the time, according to

TABLE II

Analysis of variance at the reversal rate (2f). Summary of Fourier components and their variances at the second harmonic of the stimulus frequency. Fourier component amplitude A(2f) is in microvolts, its overall variance V(2f) is in $\mu V^2$, ratio of the variance of the real part to the variance of the imaginary part $F(2f) = V_{xx}(2f)/V_{yy}(2f)$ is dimensionless, the correlation coefficient $r(2f) = V_{xy}(2f)/[V_{xx}(2f)V_{yy}(2f)]^{1/2}$ is dimensionless, and the ratio of the variance in the stimulated condition to the variance in the unstimulated condition, $V(2f)/V_0(2f)$, is dimensionless. For the variance ratios $F(2f)$ and $V(2f)/V_0(2f)$ and the amplitude A(2f), upward arrows denote values which lie in the upper 5% of their theoretical distributions, and downward arrows denote values which lie in the lower 5% tail of their distribution. For the correlation coefficient $r(2f)$, upward arrows denote values which lie in the upper 2.5% of their theoretical distributions, and downward arrows denote values which lie in the lower 2.5% tail of their distribution. Theoretical distributions are determined as described in the text.

| | Subject | | | | | | | |
|---|---|---|---|---|---|---|---|---|
| | BF | AV | AD | XA | TA | AA | SA | JV |
| *f = 5.006 Hz* | | | | | | | | |
| A(2f) | 2.418↑ | 0.972↑ | 10.129↑ | 4.531↑ | 2.374↑ | 2.884↑ | 1.975↑ | 3.745↑ |
| V(2f) | 0.225 | 0.051 | 1.780 | 0.671 | 0.490 | 0.817 | 0.093 | 0.448 |
| F(2f) | 1.273 | 0.545 | 1.738 | 2.273 | 2.684 | 0.819 | 1.325 | 0.629 |
| r(2f) | 0.078 | −0.023 | −0.513 | 0.103 | 0.307 | −0.103 | −0.465 | 0.460 |
| $V(2f)/V_0(2f)$ | 1.813 | 0.886 | 2.146 | 4.572↑ | 3.159↑ | 0.986 | 0.527 | 4.792↑ |
| *f = 7.509 Hz* | | | | | | | | |
| A(2f) | 0.567↑ | 0.335↑ | 10.463↑ | 1.661↑ | 0.607↑ | 1.306↑ | 0.080 | 3.023↑ |
| V(2f) | 0.051 | 0.112 | 1.483 | 0.119 | 0.241 | 0.189 | 0.121 | 0.282 |
| F(2f) | 1.684 | 0.836 | 1.455 | 0.202↓ | 0.882 | 0.294 | 0.833 | 5.432↑ |
| r(2f) | 0.011 | 0.395 | 0.795↑ | 0.193 | 0.701 | 0.166 | −0.210 | −0.576 |
| $V(2f)/V_0(2f)$ | 1.154 | 6.883↑ | 3.884↑ | 2.420 | 5.171↑ | 5.995↑ | 3.202↑ | 5.061↑ |
| *f = 10.012 Hz* | | | | | | | | |
| A(2f) | 0.925↑ | 0.096 | 7.639↑ | 0.618↑ | 1.236↑ | 2.221↑ | 2.154↑ | 2.297↑ |
| V(2f) | 0.045 | 0.086 | 1.093 | 0.071 | 0.297 | 0.348 | 0.488 | 0.273 |
| F(2f) | 0.250↓ | 0.323 | 0.695 | 1.731 | 1.483 | 0.432 | 0.852 | 5.066↑ |
| r(2f) | −0.220 | 0.241 | 0.828↑ | 0.335 | 0.318 | 0.469 | −0.761↓ | 0.459 |
| $V(2f)/V_0(2f)$ | 3.522↑ | 3.419↑ | 4.862↑ | 2.895↑ | 7.145↑ | 17.832↑ | 4.310↑ | 11.341↑ |

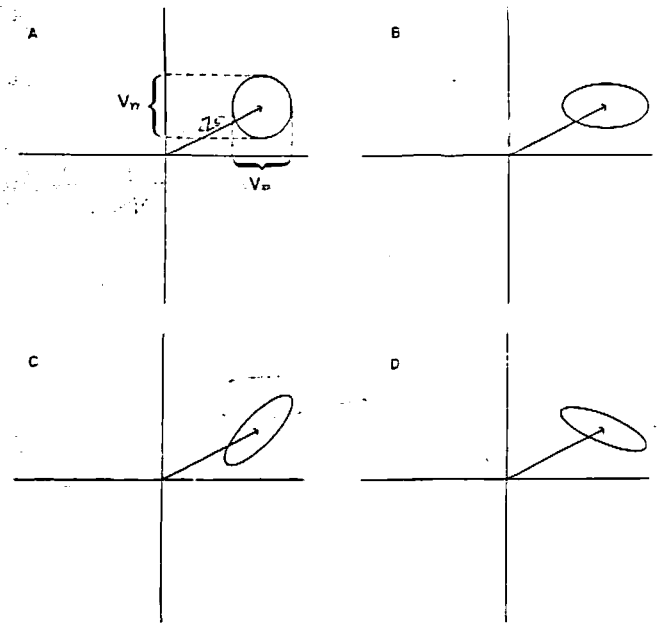


Fig. 3. Confidence regions and Fourier components. A Fourier component $\langle z_S \rangle$ may be regarded as a vector in the complex plane, whose length represents the magnitude of the Fourier component and whose direction represents the phase of the Fourier component. $V_{xx}$ denotes the variance of the real part of a Fourier estimate and $V_{yy}$ denotes the variance of the imaginary part of a Fourier estimate; their ratio $V_{xx}/V_{yy}$ is denoted by F. In addition to $V_{xx}$ and $V_{yy}$, $r = V_{xy}/(V_{xx}V_{yy})^{1/2}$ is required to characterize the shape of the confidence region. A shows the confidence region for a Fourier estimate in the situation that the real and imaginary parts of the estimate have fluctuations which are uncorrelated ($r = 0$) and of equal variance ($F = 1$). B is an example of a confidence region with $F > 1$ and $r = 0$. C is an example of a confidence region with $F = 1$ and $r > 0$. For the typical confidence ellipse, both $F \neq 1$ and $r \neq 0$. This is shown in D.

Poisson statistics. Finally, if either $F(2f)$ or $r(2f)$ were not randomly distributed, one might expect that more extreme values would be found under conditions which produced the largest enhancement in variance $V(2f)/V_0(2f)$. As seen in Table II, this is not the case.

Thus, there are no apparent systematic deviations of $F(2f)$ or $r(2f)$ from their expected distributions. Empirically, individual estimates of the real and imaginary parts of the response are uncorrelated and of equal variance. That is, the confidence interval surrounding a Fourier estimate must conform to the diagram of Fig. 3A, rather than the alternatives shown in Fig. 3B, C, and D. This observation is key to a rigorous approach to confidence regions for Fourier components (Victor and Mast 1991).

We now examine the variance ratio $V(2f)/V_0(2f)$, which expresses the change in power at the frequency 2f in the stimulated condition, as compared to the unstimulated condition. Here, the appropriate $F$ statistic has 14 degrees of freedom in both numerator and denominator (since both numerator and denominator have 7 real and 7 imaginary components). Of the 24 measured values, 22 are in the upper 95% tail. This is not surprising, given the peaks at 2f seen in Fig. 2A–C. Across subjects, the average enhancement in power was by a factor of 1.82 for stimulation at 5 Hz, 3.72 for stimulation at 7.5 Hz, and 5.66 for stimulation at 10 Hz.

For two of the subjects, one temporal frequency elicited no detectable driven component at 2f: SA at f = 7.5 Hz, AV at f = 10 Hz. (The $T^2_{circ}$ statistic (Victor and Mast 1991) was used to assess significance of driven response components.) One proposed reason for the lack of a driven response at 2f is that two or more generators happen to cancel geometrically (Halliday and Michael 1970; Jeffreys 1971; Tyler et al. 1978). This explanation, rather than a lack of responsiveness to the stimulus frequency, is supported by the fact that both subjects had driven components at 4f, even though there was no response at 2f. Here, we emphasize that in both cases, an enhancement of the variance at 2f of a similar magnitude as that observed in other subjects was seen. The bias of $V(2f)/V_0(2f)$ to values significantly larger than 1 is therefore not simply a consequence of a driven component at this frequency. Rather, it constitutes an independent index of the effect of periodic stimulation on brain activity.

## Discussion

Methods for extraction of EPs from the background EEG traditionally consist of triggered time-domain averaging, Fourier analysis with or without frequency-domain averaging, or cross-correlation, with or without filtering (Regan 1989, pp. 43–45). All of these procedures are fundamentally linear and rely on the stimulus-locked nature of the evoked potential to distinguish it from 'noise.' In this paper, we have analyzed components of the EEG during periodic visual stimulation and compared this to the EEG activity recorded without periodic visual stimulation. The analysis procedure was based on calculation of the *variances* of Fourier estimates. This procedure is not a linear one and is thus capable of detecting EEG changes not locked to the stimulus.

We first summarize our results. (i) The presence of a periodic visual stimulus alters the spectrum of the EEG. Less variance is present in the frequency range 5–17 Hz, and more is present at frequencies below 5 Hz. Periodic stimulation at 10 Hz produces a greater effect than stimulation at 7.5 Hz or 5 Hz. (ii) There are stimulus frequency-specific changes superimposed on the overall change in the spectrum. The most prominent such change is an increase in the variance estimates at the reversal rate (2f) and its second harmonic (4f). (iii) Even though specific increases in variance occur at harmonics of the input frequency, this variance is not synchronized to the 'driven,' or traditional, VEP, as

manifest (Table II) by the chance distribution of $F(2f)$ and $r(2f)$.

All of these findings are at odds with the notion that the effect of periodic visual stimulation is to synchronize the activity of a small number of neurons, and that the bulk of brain activity, which is responsible for the background EEG, is unchanged. Previous studies have disagreed as to the nature and importance of interactions between ongoing EEG activity and evoked potentials. For example, Regan (1966) found that EP amplitudes were unchanged despite epoch-to-epoch variation of alpha amplitude of up to 15-fold, and Jones and Armington (1977) found that ongoing alpha activity did not become phase-locked to a periodic visual stimulus. On the other hand, Kaufman and Locker (1973) reported intermodulations between a stimulus flickering at 1.5 Hz and the alpha rhythm, and both Sayers et al. (1974) and Başar (1980) have postulated that EPs are generated by complex interactions between stimulus and EEG. We now turn to some possible explanations for our findings.

*Results are not due to slow trends or artifacts*

One potential explanation for our findings is that the 'driven' components of the EEG changed slowly with time, either during the course of individual 30 sec data segments or during the course of the 32 episodes required for data collection from each subject. However, there were no significant trends in VEP amplitudes, either within individual episodes or during the course of a recording session. Furthermore, although an overall amplitude change would result in the appearance of excess variance at the reversal frequency (2f), it could not explain changes in variance at frequencies such as 3f (at which there was no response) or for those subjects who had no response at 2f (SA at f = 7.5 Hz, AV at f = 10 Hz).

It is also unlikely that artifacts in the EEG recordings account for our results. The presence of artifact was minimized by several methods. Subjects were well motivated and cooperative. Stimulation runs were brief (approximately 30 sec), with ad lib. pauses between runs. The recording montage ($O_z$-$C_z$) was insensitive to blink artifacts. The raw EEG signal was visually inspected during the run, and runs were aborted if large voltage excursions were observed. Thus, we believe that the fluctuations of measured Fourier components were due primarily to neural sources. Furthermore, artifacts uncorrelated with EEG activity would likely have the effect of randomly distorting variance estimates and, thus, would tend to obliterate any systematic stimulus-dependent findings.

Another potential source of 'noise' is the digitization during data collection. After amplification, the least-significant bit of the analog-to-digital converter corresponded to 0.24 $\mu$V. To estimate the contribution of digitization noise to the measured variance, we may consider the digitization noise to be a noise of uniform distribution between $\pm 0.12$ $\mu$V. This has a variance of $(0.12)^2/3 < 0.005$ $\mu V^2$, which is insignificant for the phenomena we consider here. Furthermore, digitization noise is present equally with and without periodic stimulation and, therefore, could not result in the appearance of any undriven VEP components.

*Role of attention and related processes*

It is well known that attention to a task alters the EEG (Elul 1969). Similarly, the presence of a predictably changing visual stimulus may influence the frequency content of the background EEG. This kind of change of EEG 'state' might be a subtler version of the dramatic difference in EEG frequency content when eyes are open or closed. Although a state change is a possible basis for the overall depression in EEG power in the 5–17 Hz range during periodic visual stimulation, it is unlikely to account for changes in the EEG which are specific to particular stimulus frequencies. For example, as seen in Table I, the variance at 10 Hz is increased by stimulation at 5 Hz but not 10 Hz, while the variance at 40 Hz is increased by stimulation at 10 Hz but not 5 Hz.

Now consider the possibility that brain responsiveness changes in an irregular manner over time, and that the size of the EP elicited during a particular interval depends on the brain responsiveness during that period of time. This kind of phenomenon is suggested by the work of Başar (1980), who found evidence for a systematic dependence of transient EPs on the characteristics of the EEG background immediately preceding the stimulus. The simplest kind of response modulation would be a multiplicative one, in which the overall VEP size depends on a fluctuating brain responsiveness. This multiplicative interaction of the EP and the EEG properly predicts an increase in variance at the stimulus frequency, as we have observed. But it also predicts that the phase of the VEP is known with greater certainty than its amplitude, since the postulated multiplicative interaction would distort response size but not timing. That is, the confidence region about a Fourier estimate is predicted to be elongated along the axis of the Fourier estimate itself (Fig. 4A). This is inconsistent with the analysis of Table II: the confidence region remains a circle.

Thus, overall attentional effects on the EEG background, as well as random modulation of VEP size by a fluctuating brain responsiveness do not explain our findings. A more complex picture of VEP generation is therefore required.

*Candidate models for the undriven VEP component*

Although modulation of overall response amplitude cannot explain an increase in variance without an elon-

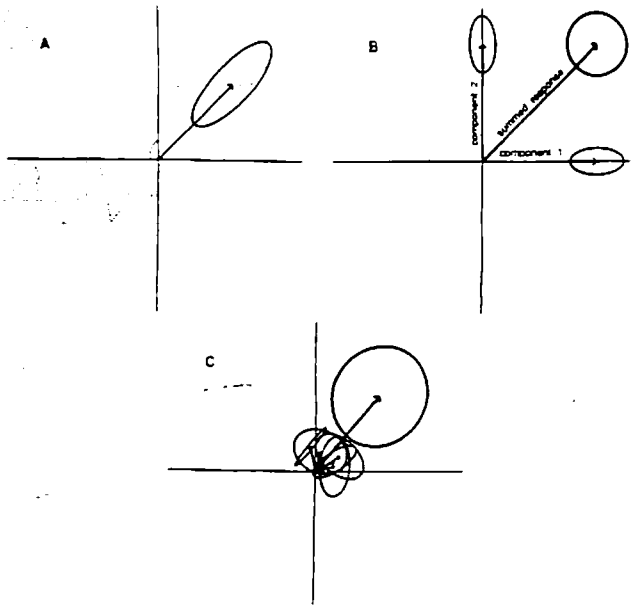


Fig. 4. Confidence regions and Fourier estimates for some models of the undriven VEP component. If the increased variance at the reversal frequency 2f were due to a multiplicative interaction with a fluctuating responsiveness, then the confidence ellipse would be elongated along the direction of the Fourier estimate (A). A superposition of two components in quadrature, each of which has an independent but identical multiplicative noise, yields a response whose confidence region is circular (B). A superposition of many components each with their own confidence regions may lead to a net response with a nearly circular confidence region (C).

gation of the confidence region, a simple elaboration on this model can account for this finding. Let us assume that the driven VEP has two independent neural generators, which produce driven components at relative phase of $\pi/2$ radians (90°; Fig. 4B). Further, assume that the fluctuations of these components are modulated in a multiplicative fashion, and that these fluctuations are equal in expected size, but statistically independent. If either component were recorded alone, we would recover the situation illustrated in Fig. 4A. Now consider the superposition of these two components, and their respective variances. The driven components and their variances $V_{xx}$, $V_{yy}$, and $V_{xy}$ sum linearly, because variances of independent processes add. It follows that the confidence interval for the combined response is circular.

The orientations of the Fourier estimates themselves are irrelevant to the above analysis. Other than independence of component variances, the crucial features in the above model are that the confidence regions about the two components have orthogonal major axes, and that these ellipses are of the same size and shape. It seems relatively unlikely that this would occur for most subjects under most conditions.

Although the 2-component model of Fig. 4B relies on coincidences to achieve a circular confidence region, it does illustrate an important point: components with elliptical confidence regions may combine additively to form a response whose confidence region is more nearly circular, without cancellation of the driven EP.

The multiplicative interaction we have considered is only one way to generate interactions between background EEG and the EP. In general, any non-linear oscillator (Kaufman and Locker 1973; Wilson and Cowan 1973; Kawahara 1980) driven both by an EP signal and noise will lead to interactions between the EP and the 'noise,' and hence a change in the variance of Fourier components at the response frequency 2f. The shape and orientation of the confidence region will depend on the details of the oscillator's dynamics. Now consider the possibility that the VEP is generated by not just two components, but many components. The confidence regions for each component will be ellipses with different eccentricities and orientations (Fig. 4C). However, if there are enough ellipses of different orientations, the net confidence region obtained by superimposing the components is likely to be roughly circular.

The crucial part of this analysis is that it is 'easier' for the eccentricities of confidence regions to cancel than for the driven components themselves to cancel. This is because rotation of an ellipse by only 90° leads to cancellation (Fig. 4B) of eccentricities, while rotation of the response vector by 180° is required for cancellation. Conversely, synchronization of driven EP components may be relatively crude (i.e., within 180°), and a net driven EP will result. However, the uncertainty ellipses must be within 90° of a common phase to avoid cancellation.

*Changes in the variance at the stimulus repeat frequency*

Because of the symmetry of the pattern-reversal stimulus, we do not anticipate any driven EP components at the stimulus repeat frequency f. In broadest terms, this is because a single reversal of the stimulus is equivalent to a translation of the stimulus. Since scalp recording sums over a wide region of cortex, such translations cannot yield a net driven response.

The simple cells (De Valois et al. 1979) of primary visual cortex and likely other cell types as well) are anticipated to be driven at the fundamental frequency f. Even though symmetry forbids recording their net signal as a driven EP, the analysis above would suggest that periodic activation of these neurons will lead to increased variance at f. However, in contrast to the fairly large variance increases seen at 2f and 4f (Table I), there is little if any increase in variance at f. (Increased variance at f might also be manifest as 'period-doubling,' which appears to be evanescent and rarely substantial (Regan 1972, p. 236).) One possibility for the apparent lack of a variance increase at the fundamental frequency f is that it, also, it cancelled by the same symmetry considerations which cancel the driven response at f. We point out that this can only occur if

the 'noise' sources are highly correlated over a cortical scale corresponding to the check size.

*Changes in the variance at other harmonics*

The analysis above does not address the changes in power that appear at a range of integer harmonics (kf) of the input frequencies (Table I). It is interesting to note that the largest changes in variance occur at around 20 Hz, independent of whether this frequency is the second harmonic of the input frequency (f = 10 Hz) or the fourth harmonic of the input frequency (5 Hz). At present, we display these data as a future basis for evaluation of specific non-linear models and do not attempt to draw additional qualitative inferences from them.

*Conclusion*

We have shown that a periodic visual pattern induced changes in the EEG in addition to the traditional 'driven' EP. The nature of these interactions provides a new insight into the complexity of mechanisms that underlie EP generation.

Previously, there has been relatively little evidence for interactions between steady-state VEP signal and the ongoing EEG (Van der Tweel and Verduyn Lunel 1965; Regan 1966; Kaufman and Locker 1973). Since some of the phenomena we have observed are not small (e.g., a 6-fold increase in variance), we suspect that EP/EEG interactions are not well appreciated simply because routine data collection techniques strive to obliterate them.

## Appendix: characteristics of fluctuations of Fourier components

Here we examine the Fourier components $z_S(\omega,L,T)$ in greater detail. The main goal is to understand how variances and covariances of the real and imaginary parts of $z_S$ behave under the hypothesis (8) that the scalp signal is a sum of two components: an evoked response R(t), and ongoing 'noise' unrelated to the stimulus E(t). This Appendix also calculates the covariances of Fourier components $z_S(\omega,L,T)$ and $z_S(\omega,L,T')$ obtained at successive times.

To address the issue of the covariances of the Fourier components, we must postulate some form for the 'noise' term E(t). We will assume that E(t) is represented by a gaussian, though not necessarily white, noise of mean zero (Elul 1969). Therefore, E(t) is completely described by its autocorrelation function A(h), which is defined as

$$A(h) = \langle E(\tau)E(\tau + h)\rangle \qquad (13)$$

The autocorrelation function is symmetric:

$$A(h) = A(-h).$$

We are interested in the distribution of the deviations of individual estimates $z_S(\omega,L,T)$ from their expected values $\langle z_S(\omega,L,T)\rangle$, denoted by $\delta z_S(\omega,L,T)$. For simplicity, we will assume that we have sufficient data so that we may approximate $\langle z_S(\omega,L,T)\rangle$ by its sample estimate $\langle z_S(\omega,L,T)\rangle_{est}$. As shown by equation (10) above, $\delta z_S(\omega,L,T)$ depends only on the 'noise' term E(t):

$$\delta z_S(\omega,L,T) = \int_{-\infty}^{\infty} E(t)\, W(t-T)\, e^{-i\omega t}\, dt \qquad (14)$$

where W(t) again denotes the windowing function, such as eqn. (2).

The real and imaginary parts of (14), $\delta x_S(\omega,L,T)$ and $\delta y_S(\omega,L,T)$, are distributed in a gaussian fashion (because they are linear superpositions (14) of gaussian-distributed quantities) and have a mean of zero. Thus, their joint distribution is completely determined by their variances and covariances.

We examine the covariance of the fluctuation of an estimate at the frequency $\omega = 2n\pi/P$ at time T, and the fluctuation of a second estimate at the frequency $\omega' = 2n'\pi/P$ at time T'. It is helpful to express all times other than T, the midpoint of the first interval, in terms of new variables as follows: (i) $D = T' - T$, the time between the midpoints of the two intervals used for estimates: (ii) $\tau = t - T$, time relative to the midpoint of the first interval; and (iii) $h = (t' - T') = \tau$, time relative to the midpoint of the second interval minus $\tau$.

With this change of variables, the covariance of fluctuations of the real parts of 2 estimates (14) is:

$$\begin{aligned}
&\langle \delta x_S(\omega,L,T)\ \delta x_S(\omega',L,T')\rangle \\
&= \Big\langle \iint_{-\infty}^{\infty} E(t)E(t')\, W(t-T)\, W(t'-T')\cos(\omega t) \\
&\quad \times \cos(\omega' t')\, dt\, dt' \Big\rangle \\
&= \tfrac{1}{2}\Big\langle \iint_{-\infty}^{\infty} E(T+\tau)E(T+\tau+h+D)\, W(\tau)\, W(\tau+h) \\
&\quad \times \{\cos[\omega(T+\tau) + \omega'(T+\tau+h+D)] \\
&\quad + \cos[\omega(T+\tau) - \omega'(T+\tau+h+D)]\}\, d\tau\, dh \Big\rangle.
\end{aligned} \qquad (15)$$

This expression now may be simplified. Fluctuations of the 'noise' E(t) are independent of the remaining quantities (W(t) and the cosine terms) in (15). Thus, in the calculation of the ensemble-average $\langle\ \rangle$ in (15), $E(T+\tau)E(T+\tau+h+D)$ can be replaced by its expected value A(h + D), as given by (13). This leads to

$$\begin{aligned}
&\langle \delta x_S(\omega,L,T)\ \delta x_S(\omega',L,T')\rangle \\
&= \tfrac{1}{2}\Big\langle \iint_{-\infty}^{\infty} A(h+D)\, W(\tau)\, W(\tau+h) \\
&\quad \times \{\cos[\omega(T+\tau) + \omega'(T+\tau+h+D)] \\
&\quad + \cos[\omega(T+\tau) - \omega'(T+\tau+h+D)]\}\, d\tau\, dh \Big\rangle
\end{aligned} \qquad (16)$$

The expected value $\langle\ \rangle$ is an average over an ensemble of repetitions of the experiment. Since it only depends on the 'noise' E(t), it must be independent of the absolute time T chosen for the first interval. This can only happen if the above expression is zero, or if $\omega' = \omega$ or $\omega = -\omega'$. In these cases, we find

$$\langle \delta x_S(\omega,L,T)\ \delta x_S(\pm\omega,L,T')\rangle$$
$$= \tfrac{1}{2}\int\!\!\int_{-\infty}^{\infty} A(h+D)\ W(\tau)\ W(\tau+h) \times \cos[\omega(h+D)]\ d\tau\ dh \quad (17)$$

A similar argument leads to

$$\langle \delta y_S(\omega,L,T)\ \delta y_S(\pm\omega,L,T')\rangle$$
$$= \pm\tfrac{1}{2}\int\!\!\int_{-\infty}^{\infty} A(h+D)\ W(\tau)\ W(\tau+h) \times \cos[\omega(h+D)]\ d\tau\ dh \quad (18)$$

and

$$\langle \delta x_S(\omega,L,T)\ \delta y_S(\pm\omega,L,T')\rangle$$
$$= \pm\tfrac{1}{2}\int\!\!\int_{-\infty}^{\infty} A(h+D)\ W(\tau)\ W(\tau+h) \times \sin[-\omega(h+D)]\ d\tau\ dh \quad (19)$$

We first focus on estimates from the same interval ($T = T'$, $D = 0$), and then for distinct intervals. When both estimates are from the same interval ($T = T'$ and $D = 0$), the covariance of the real and imaginary part of the fluctuation is zero, because of the symmetry of the function A(h). Furthermore, the variances

$\langle \delta x_S(\omega,L,T)\ \delta x_S(\pm\omega,L,T)\rangle$ (equation (17))

and $\pm\langle \delta y_S(\omega,L,T)\ \delta y_S(\pm\omega,L,T)\rangle$ (equation (18))

of fluctuations of the Fourier coefficients estimated from an interval of length L are equal. We denote this quantity by V(L)/2, with

$$V(L) = \int\!\!\int_{-\infty}^{\infty} A(h)\ W(\tau)\ W(\tau+h)\ \cos(\omega h)\ d\tau\ dh \quad (20)$$

The results thus far may be summarized as follows: fluctuations of the estimates of Fourier components are gaussian-distributed quantities of mean zero, and may therefore be characterized completely by their variances and covariances. Fluctuations in the estimates of Fourier components at two frequencies $\omega$ and $\omega'$ are independent unless the frequencies coincide ($\omega = \pm\omega'$). When the frequencies do coincide, the covariance of the fluctuations in the real parts (17) and imaginary parts (18) are equal. Covariances of fluctuations in estimates from two intervals depend on the time interval D between the two data samples used for the estimate, and on the autocorrelation function of the noise process, but *not* on the evoked response R(t). In the special case that the two intervals coincide, fluctuations in the real and imaginary portions of the estimates are uncorrelated, and their total variance is given by V(L) (equation 20).

To understand the relationship between the covariances and the separation D between the two intervals, we transform the expressions (17), (18), and (19) into the frequency domain. For this purpose, expressions (17) and (19) are conveniently combined into a common expression:

$$\langle \delta x_S(\omega,L,T)\ \delta z_s(\omega,L,T')\rangle$$
$$= \langle \delta x_S(\omega,L,T)\ \delta x_S(\omega,L,T')\rangle + \iota\langle \delta x_S(\omega,L,T)\ \delta y_S(\omega,L,T')\rangle$$
$$= \tfrac{1}{2}\int\!\!\int_{-\infty}^{\infty} A(h+D)\ W(\tau)\ W(\tau+h) e^{-\iota\omega(h+D)}\ d\tau\ dh \quad (21)$$

Application of the convolution formula for Fourier transforms to (21) yields

$$\langle \delta x_S(\omega,L,T)\ \delta z_S(\omega,L,T')\rangle$$
$$= 2\pi^2\int_{-\infty}^{\infty} \tilde{A}(\omega+\phi)\,|\tilde{W}(\phi)|^2\, e^{\iota\phi D}\, d\phi \quad (22)$$

where $\tilde{A}(\phi)$ and $\tilde{W}(\phi)$ are the Fourier transforms of A(h) and W(h):

$$\tilde{A}(\phi) = \frac{1}{2\pi}\int_{-\infty}^{\infty} A(h)\, e^{-\iota\phi h}\, dh;\quad A(h) = \int_{-\infty}^{\infty} \tilde{A}(\phi)\, e^{\iota\phi h}\, d\phi \quad (23)$$

and

$$\tilde{W}(\phi) = \frac{1}{2\pi}\int_{-\infty}^{\infty} W(h)\, e^{-\iota\phi h}\, dh;$$
$$W(h) = \int_{-\infty}^{\infty} \tilde{W}(\phi)\, e^{\iota\phi h}\, d\phi. \quad (24)$$

The expression (22) can be approximated if the power spectrum $\tilde{A}$ may be regarded as approximately flat in the vicinity of $\omega$. For a sampling window W of length L, only frequencies $\phi$ which are small in comparison to $2\pi/L$ contribute to the integral (22) because of the windowing term $|\tilde{W}(\phi)|^2$. Thus, for sufficiently large L, we may approximate the covariances (22) by

$$\langle \delta x_S(\omega,L,T)\ \delta z_S(\omega,L,T')\rangle$$
$$= 2\pi^2\,\tilde{A}(\omega)\int_{-\infty}^{\infty} |\tilde{W}(\phi)|^2\, e^{\iota\phi D}\, d\phi$$
$$= \pi\,\tilde{A}(\omega)[W * W](D), \quad (25)$$

where $[W \times W](t)$ is the convolution of the window function (2) with itself:

$$[W * W](t) = (L - |t|)/L^2 \text{ if } |t| \leq L;$$
$$[W * W](t) = 0, \text{ otherwise.} \quad (26)$$

Thus, the variances and covariances (25) of the fluctuations of estimates of Fourier components are

approximated by a product of two terms. One term, $\tilde{A}(\omega)$, is the amount of power in the 'noise' near the frequency of interest $\omega$. The second term, $[W \times W](D)$, expresses the extent of overlap of two window functions separated in time by D. In general, since $[W * W](t)$ is zero for all arguments outside of the range $[-L, L]$, estimates of Fourier components from non-overlapping intervals ($|D| > L$) are essentially independent. This approximation is valid provided that L is large enough so that the power spectrum $\tilde{A}(\cdot)$ is approximately flat within a frequency window $2\pi/L$ about $\omega$.

We have seen that if the data interval L is sufficiently long, then spectral estimates from non-overlapping segments are independent. This is exactly the same criterion for L that ensures that the power spectrum, as rigorously defined by the limiting process (5), is adequately approximated by an estimate obtained from a finite value of L. To see this, we specialize (25) to $T = T'$. We find

$$\begin{aligned} \langle |\delta z_S(\omega, L, T)|^2 \rangle &= 4\pi^2 \tilde{A}(\omega) \int_{-\infty}^{\infty} |\tilde{W}(\phi)|^2 \, d\phi \\ &= 2\pi \tilde{A}(\omega) [W * W](0) \\ &= 2\pi \tilde{A}(\omega)/L. \end{aligned} \tag{27}$$

It follows immediately from (5) that if the approximation (25) is valid, then the power spectrum $\hat{S}(\omega)$ is the Fourier transform of the autocorrelation of the noise process $\tilde{A}(\omega)$.

This work was supported in part by Grants EY1428, EY6871, EY7977, and HD819.

We thank Mary Conte and Annemarie Canel for their assistance.

## References

Başar, E. EEG-Brain Dynamics: Relation Between EEG and Brain Evoked Potentials. Elsevier, Amsterdam, 1980.

De Valois, K.K., De Valois, R.L. and Yund, E.W. Responses of striate cortex to grating and checkerboard patterns. J. Physiol. (Lond.), 1979, 291: 483–505.

Elul, R. Gaussian behavior of the electroencephalogram: changes during performance of mental task. Science, 1969, 164: 328–331.

Halliday, A.M. and Michael, W.F. Changes in pattern-evoked responses in man associated with the vertical and horizontal meridians of the visual field. J. Physiol. (Lond.), 1970, 208: 499–513.

Jeffreys, D.A. Cortical source locations of pattern related VEPs recorded from the human scalp. Nature, 1971, 229: 502–504.

Jones, K.G. and Armington, J.C. The removal of alpha from the VECP by means of selective averaging. Vision Res., 1977, 17: 949–956.

Kaufman, L. and Locker, Y. Sensory modulation of the EEG. In: Proc. American Psychological Association, 75th Meeting, 1969: 179–180.

Kawahara, T. Coupled Van der Pol oscillators — a model of excitatory and inhibitory neural interactions. Biol. Cybernet., 1980, 39: 37–43.

Kay, S.M. Modern Spectral Estimation. Prentice-Hall, Englewood Cliffs, NJ, 1988.

Mikkman, N., Schick, G., Rossetto, M., Ratliff, F., Shapley, R. and Victor, J.D. A two-dimensional computer-controlled visual stimulator. Behav. Res. Meth. Instrum., 1980, 12: 283–292.

Regan, D. Some characteristics of average steady-state and transient responses evoked by modulated light. Electroenceph. clin. Neurophysiol., 1966, 20: 238–248.

Regan, D. Evoked Potentials in Psychology, Sensory Physiology, and Clinical Medicine. Wiley, New York, 1972.

Regan, D. Human Brain Electrophysiology, Elsevier, New York, 1989.

Sayers, B.McA., Beagley, H.A. and Henshall, W.R. Mechanism of auditory evoked responses. Nature, 1974, 247: 481–483.

Sokal, R.R. and Rohlf, F.J. Biometry: The Principles and Practice of Statistics in Biological Research. Freeman, San Francisco, CA, 1969.

Tyler, C.W., Apkarian, P.A. and Nakayama, K. Multiple spatial frequency tuning of electrical responses from the human visual cortex. Exp. Brain Res., 1978, 33: 535–550.

Van der Tweel, L.H. and Verduyn Lunel, H.F.E. Human visual responses to sinusoidally modulated light. Electroenceph. clin. Neurophysiol., 1965, 18: 587–598.

Victor, J.D. and Mast, J. A new statistic for steady-state evoked potentials. Electroenceph. clin. Neurophysiol., 1991, 78: 378–388.

Wilson, H.R. and Cowan, J.D. A mathematical theory of the functional dynamics of cortical and thalamic nervous tissue. Kybernetik, 1973, 13: 55–80.